Phonon properties of (311) GaAs/AlAs superlattices

Z. V. Popović, E. Richter,* J. Spitzer, M. Cardona, A. J. Shields,† R. Nötzel, and K. Ploog‡
Max-Planck-Institut für Festkörperforschung, Heisenbergstrasse 1, D-70569 Stuttgart, Federal Republic of Germany
(Received 16 August 1993)

Raman scattering spectra of GaAs/AlAs superlattices grown along the [311] direction are compared with results of lattice-dynamical calculations. Confined optical as well as folded acoustic-phonon modes are clearly observed at frequencies in excellent agreement with those predicted. Several of the bulk branches hybridize along the low-symmetry [311] direction, producing confined optical modes in the superlattice of mixed longitudinal/transverse character. This hybridization complicates also the assignment of a mode order to the confined phonons, since they encompass components deriving from several bulk branches with different effective wave vectors. We demonstrate that a proper assignment can only be made by comparison to the calculated eigenvector envelope functions. We discuss how the crystal symmetry affects the angular dispersion of the optic modes.

I. INTRODUCTION

There has been considerable interest in the electronic properties of GaAs/AlAs superlattices (SL's) grown on (311)-oriented substrates.[1–7] Reflection high-energy diffraction measurements and high-resolution transmission-electron microscopy[4] indicate the surface to be corrugated with a 32 Å period. It was suggested that an inversion of the GaAs and AlAs growth surfaces leads to the formation of a SL where the layer widths vary periodically along one of the lateral directions. This quasi-one-dimensional layer structure was invoked to explain the observed redshift of the band edge exciton of (311) SL's compared to their simultaneously grown (100) counterparts.[4]

There have also been several investigations of (311)-oriented GaAs/AlAs SL's using Raman spectroscopy.[8–10] These SL's provide the rare opportunity of observing folded phonons arising from all three acoustic branches.[8] The optic-phonon modes have also been studied, both for laser energies close to resonance with the band edge,[9] as well as higher-energy electronic transitions.[10] Near resonance with the SL band edge a splitting of the Raman peak due to each confined longitudinal optical (LO) mode was observed and ascribed to a finite in-plane wave vector induced by the lateral periodicity.[9] Close to resonance with the transition between the second electron and heavy hole subbands it was shown that an intraband deformation potential mechanism, forbidden in (100) SL's, contributes to the scattering intensity.[10]

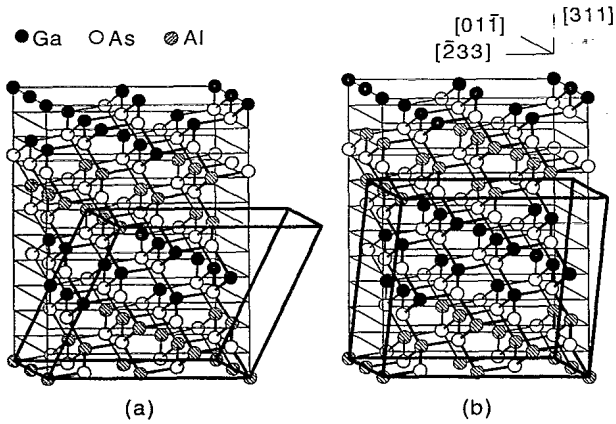

FIG. 1. Schematic of the crystal structure of (a) $(GaAs)_3/(AlAs)_3$ (space group B_σ) and (b) $(GaAs)_4/(AlAs)_3$ (space group P_σ) (311) SL's . The nearest neighbor bondings are indicated by thicker lines. The thickest lines indicate the edges of the SL unit cell.

In this paper we compare Raman scattering spectra of both the optic and acoustic regions to lattice-dynamical calculations of the vibrational frequencies of SL's grown along the [311] direction. Emphasis is placed on the polarization mixing and angular dispersion of the SL modes.

Figure 1 illustrates the atomic configuration in (311) GaAs/AlAs SL's. The structure is built up by pairs of anion and cation planes perpendicular to the SL axis, with a monolayer spacing of $a = a_0/\sqrt{11} = 1.7$ Å. Each cation (anion) plane is neighbored on one side by a rather close anion (cation) plane (separated by $a/4$) and on the other by a more distant one ($3a/4$). The (311) SL's have monoclinic symmetry with point group C_s, for which there is only one symmetry operation, a mirror plane σ perpendicular to the [01$\bar{1}$] direction, apart from the identity element. The corresponding space group depends on the number of monolayers: for an even number, the SL has a B-face centered space group Bm (C_s^3), while for an odd number, the space group is primitive Pm (C_s^1). These two types of crystal structures are shown in Figs. 1(a) and 1(b).

II. LATTICE DYNAMICS

Lattice-dynamical calculation were performed for the (311) $(GaAs)_{17}/(AlAs)_{17}$ SL using the shell model previ-

ously applied to (012),[11,12] (110),[13] and (111) (Ref. 14) GaAs/AlAs SL's with parameters fitted to neutron data for GaAs.[15] The mass approximation was used for the AlAs layers (all lattice-dynamical parameters taken to be the same as for GaAs, except for the mass). The interface roughness and corrugation[4] of the layers was ignored.

In the (311) SL's the lowering of the symmetry from the cubic bulk structure to a monoclinic crystal (point group C_s) leads to a more complicated lattice dynamical behavior than in the (001) and (111) cases. Compared with other low-symmetry SL's, such as those grown along (012) and (110),[12,13] the lattice dynamics properties of (311) SL's are similar to the (110) case (point group C_{2v}). As for (110) SL's, the SL modes propagating parallel to the growth direction ([311]) are either purely transverse (labeled A''), when polarized parallel to $[01\bar{1}]$ (x' direction), or have mixed longitudinal/transverse character (A'). This classification remains valid for nonvanishing wave vectors along the [311] direction. However, in contrast to the (110) case, there is no symmetry element in C_s which would allow a classification of the modes in terms of even and odd parity with respect to the center plane of the layers. Another similarity with the (110) case is that the bulk dispersion curves along the [311] direction of the two SL constituents do not decrease monotonically, as evident in Fig. 2, due to an anticrossing of the modes with the same symmetry (A') with respect to the point group of $\vec{q}$.

As usual we analyze the optical mode frequencies calculated for the (311) SL's by defining an effective wave vector related to the confinement to either the GaAs or AlAs layers,

$$q_m = \frac{m\pi}{d_i} \quad \text{with } d_i = (n_i + \delta)\frac{a_0}{\sqrt{11}}, \qquad (1)$$

where $a_0/\sqrt{11}$ is the thickness of one monolayer and n_i the number of GaAs (or AlAs) monolayers, respectively. The value of the "quantum defect" δ describes the penetration of the modes into the other layer.

In Fig. 2 we compare the frequencies calculated for a $(GaAs)_{17}/(AlAs)_{17}$ SL plotted as a function of their effective wave vector given by Eq. (1) with the bulk mode dispersions along [311]. Since the purely transverse optical (TO) modes polarized along x' [labeled $\omega_2(k)$ in Fig. 2] do not mix with any other branch, they have just one effective wave vector. For the $TO_{x'}$ branch we find the best mapping of the calculated frequencies onto the bulk dispersion by taking $\delta = 1$, as plotted in Fig. 2(a) for the GaAs region. This is consistent with the vibrations extending to the first cation in the barriers on either side of the layer.[16] As an example, the displacement vector components of the $TO_{x',1}$ mode are given in Fig. 3(g).

The mapping of the calculated vibrational frequencies of the SL onto the bulk dispersion is more complicated for the A' modes due to their strongly mixed character. First, $LO_{z'}$ and $TO_{y'}$ hybridize strongly at the frequencies where their bands overlap. Furthermore, as can be seen in Fig. 2, there is also a strong mixing of the $LO_{z'}$ with a transverse acoustic branch at larger wave vectors. This hybridization complicates the assignment of an effective wave vector to each mode, since they in general en-

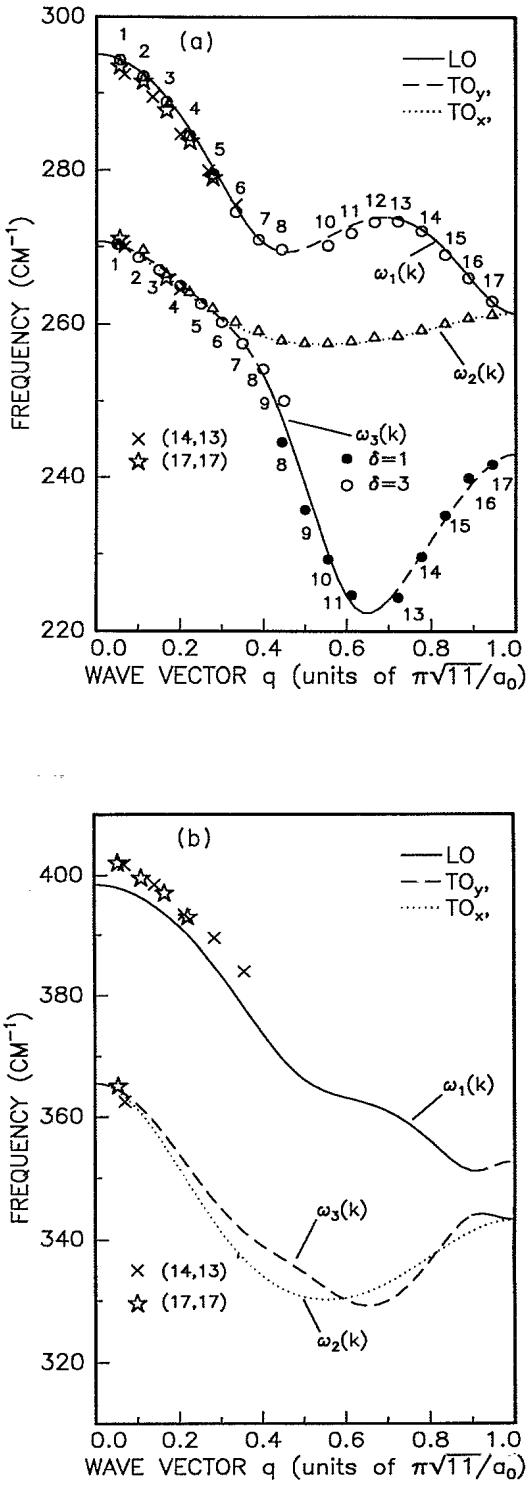

FIG. 2. Experimental and calculated confined mode frequencies of a (311) $(GaAs)_{17}(AlAs)_{17}$ superlattice as a function of confinement wave vector $\vec{q}_m$, Eq. (1), together with theoretical optical-phonon dispersion curves of bulk (Ref. 15) (a) GaAs and (b) AlAs in the [311] direction. The dominant LO/TO character is indicated. The "quantum defect" δ was taken to be either one or three, as given in the figure. The stars and crosses represent measured frequencies while the circles and triangles give the results of the superlattice calculations.

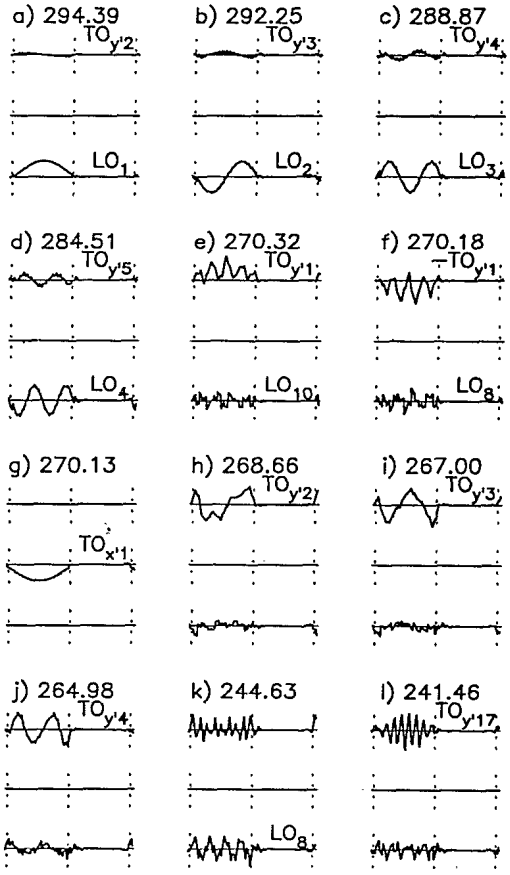

FIG. 3. Envelope functions for a number of GaAs-like optical relative-displacement vectors of anion-cation pairs at the zone center of the $(GaAs)_{17}/(AlAs)_{17}$ (311) SL for $\vec{q}_m \to 0$ along the layer axis. The numbers denote the corresponding frequency in cm^{-1}.

compass components from the mixed bulk branches with *different* effective wave vectors. Since the effective wave vectors which correspond to different branches but to the same mode frequencies have quite different magnitudes and are incommensurate, they can shift the frequencies to lower or higher values compared to the bulk case.[12]

In contrast to (311) SL's, (110) SL's possess a reflection plane perpendicular to the growth axis. Therefore the envelope functions of the LO_m and TO_m components have different parity with respect to a reflection at the middle of the layers and $LO_{m=\text{even (odd)}}$ mix only with $TO_{m=\text{odd (even)}}$.[13] However, even for (311) SL's, in the limit of small q_m's one can show that within the macroscopic formulation of Ref. 17 a similar reflection plane approximately exists. Hence for small m we expect strong admixtures only of LO and TO modes with opposite parity, i.e., $LO_{m=\text{even}}$ with $TO_{m=\text{odd}}$ and $LO_{m=\text{odd}}$ with $TO_{m=\text{even}}$.

Using the definition of Eq. (1) for the effective wave vector, the calculated and measured SL frequencies are found to map the bulk dispersions most closely for the following.

(a) $\delta = 1$ for the $\omega_1(k)$ branch. Displacement vector components for modes of this kind are shown in Figs. 3(a)–3(d). As can be seen from Fig. 2(a), the LO_9 mode is missing, but two $TO_{y',1}$ modes appear. These modes show considerable admixture with large q_m modes ($q_m \approx 8 - 10$) as shown in Figs. 3(e) and 3(f).

(b) $\delta = 3$ for the upper part of the $\omega_3(k)$ branch. In the frequency region between 270 cm^{-1} and 245 cm^{-1} ($0 \le q \le 0.45$) we find the closest mapping for $\delta = 3$. This arises from the hybridization of the $LO_{z'}$ and $TO_{y'}$ modes, which pushes the $TO_{y'}$ modes to lower wave vector in a manner that can be modeled by an increase in δ. The displacement vector components of the $TO_{y'}$ (for $m = 1 - 4$) modes are given in Figs. 3(e) and 3(h)–3(j).

(c) $\delta = 1$ for the lower part of the $\omega_3(k)$ branch. For $0.45 \le q \le 0.65$ the $\omega_3(k)$ branch is the nearly unmixed continuation of the $\omega_1(k)$ branch (eigenvector exchange) and $\delta = 1$ can be taken again. The corresponding modes are labeled $m = 8$, 9, 10, and 11. Displacement eigenvector components for this kind of modes are shown in Fig. 3(k) for $m = 8$. The discontinuity in the calculated frequencies near 245 cm^{-1} in Fig. 2(a) is due the abrupt change of δ from 3 to 1 used to obtain good mapping of the SL frequencies to the bulk dispersions. For $0.65 \le q \le 1$ another eigenvector exchange with the dominantly transverse-acoustic branch section takes place. As an example, the displacement vector components of $TO_{y',17}$ are given in Fig. 3(l).

The low C_s symmetry of the (311) SL's is also reflected in the angular dispersion of the near-zone-center modes ($\vec{q} \to \vec{0}$) as demonstrated in Fig. 4. Due to the fact that the $[\bar{2}33]$ and $[01\bar{1}]$ directions are not symmetry equivalent, the dispersion curves and eigenvectors of corresponding modes are different for wave vectors parallel to these two in-plane directions. It is known that only modes which are infrared-active along the direction of propagation exhibit angular dispersion.[12] In the case of (311) SL's all the modes (A' and A'') are infrared active, although not necessarily along the direction of propagation.

In the left-hand side of Fig. 4 the wave vector $\vec{q}$ is rotated in the z'-y' ($01\bar{1}$) plane. Since the electric dipole

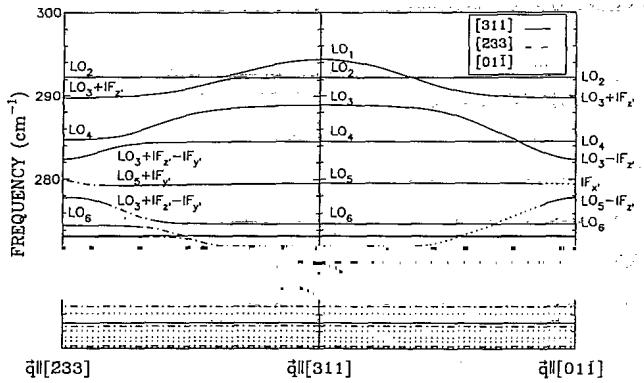

FIG. 4. Calculated angular dispersion of the optical modes of a $(GaAs)_{17}/(AlAs)_{17}$ SL for infinitesimal q_m. In the left panel, $\vec{q}_m$ varies in the $(01\bar{1})$ plane, while in the right panel, $\vec{q}_m$ rotates in $(\bar{2}33)$. The solid, dashed, and dash-dotted lines represent modes predominantly polarized along z' (LO), x' ($TO_{x'}$), y' ($TO_{y'}$), respectively.

moment of the A'' modes is parallel to the x' ([01$\bar{1}$] direction) their frequencies are independent of the angle of propagation, while, in contrast, the A' modes do exhibit both angular dispersion and anticrossing effects. In (100) SL's, the m = even order modes have zero dipole moment along the propagation direction, due to the twofold rotation axis bisecting the layers. Consequently, only the odd order modes are found to disperse for increasing wave vector parallel to the layers. As discussed earlier, there is no such symmetry element for (311) SL's, a fact which allows both m= even and m = odd modes to be infrared active and therefore to show dispersion and anticrossing effects. However, as evident in Fig. 4, the even order modes disperse much less than the odd ones, because the "quasisymmetry" about the center plane of the layers in (311) SL's, arguable in the macroscopic approximation, results in a much smaller dipole moment for the even modes than for the odd ones.

Turning now to varying $\vec{q}$ in the ($\bar{2}33$) plane (Fig. 4, right-hand side) both the A' and A'' modes are infrared active along the direction of propagation and hence should show angular dispersion. In contrast to the previously discussed rotation in the (01$\bar{1}$) plane, we find that the A'' modes, as well as the A' ones, disperse. The A' modes with m = odd display strong angular dispersion in the frequency range between 295 cm^{-1} and 273 cm^{-1}, while the even order ones show negligible change in frequency, as well as no observable anticrossing effects: the A' modes with even m have a dipole moment parallel to the [$\bar{2}$33] axis and are therefore not affected by a variation of the wave vector within the ($\bar{2}$33) plane. Due to the fact that A' modes with even and odd m belong to the same representation anticrossings between both kinds of modes should be present in principle, but cannot be observed on the frequency scale of Fig. 4.

Figure 5 shows envelope functions of the eigenvector components for several modes with small $\vec{q}$ parallel to the layer plane. The two columns on the left show modes with $\vec{q} \parallel [01\bar{1}]$, the two on the right with $\vec{q} \parallel [\bar{2}33]$. The eigenvectors of these modes ($\vec{q} \perp [311]$) partially display a superposition of confined bulklike modes with the interface modes (IF$_{z'}$, IF$_{y'}$, and IF$_{x'}$—according to their contribution to either the z', y', or x' components of the eigenvectors) of the type obtained in the electrostatic approximation [Figs. 5(b), 5(d), 5(f), 5(i), 5(k)–5(m)]. The envelope functions of Fig. 5(e) exhibit the typical displacement pattern of an interface modes with exponentially decaying penetration into the AlAs layer and a nearly constant displacement in the GaAs layer. All other *in-plane* modes with negligible angular dispersion have the same eigenvector components as the corresponding confined modes for small $\vec{q} \parallel [311]$ and $\vec{q} = 0$ [cf. Figs. 5(a), 5(c), 5(g), 5(h) and 5(n)].

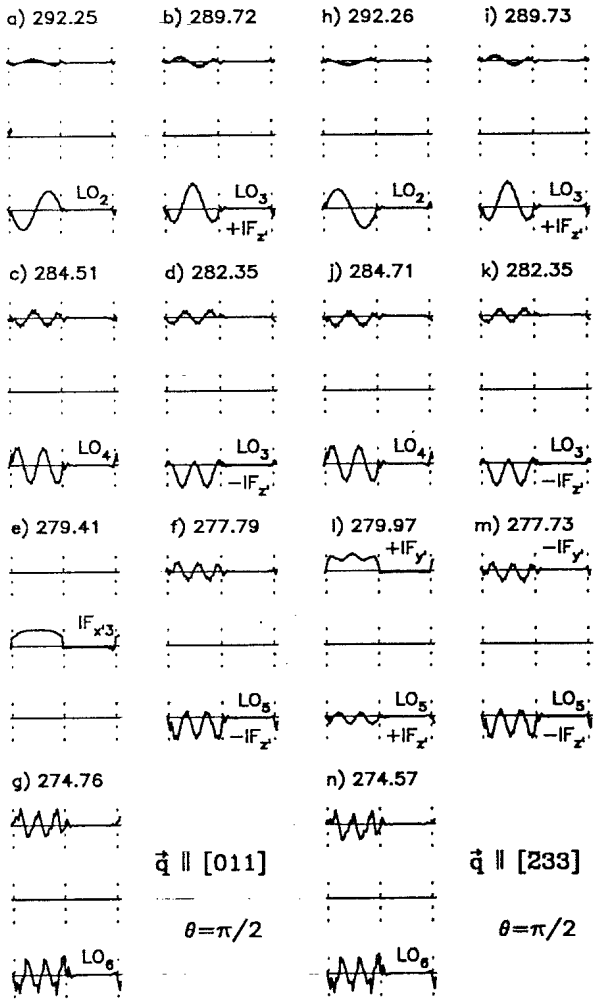

FIG. 5. Envelope functions as in Fig. 3 for a number of GaAs-like zone-center optical modes of the (GaAs)$_{17}$/(AlAs)$_{17}$ SL for $\vec{q}_m$ perpendicular to the layer axis and $\vec{q} \to \vec{0}$. Left panel $\vec{q} \parallel [01\bar{1}]$ and right panel $\vec{q} \parallel [\bar{2}33]$.

III. EXPERIMENT

The samples studied here were grown on (311)A-oriented, semi-insulating GaAs substrates by molecular-beam epitaxy under standard conditions, i.e., growth rate 0.3–1.2 μm/h, group V to group III flux ratio 5:1, and substrate temperature 580–620 °C. Details of the growth procedure and x-ray characterization of the samples have been given earlier.[4] As an illustration of the sample quality, Fig. 6 shows the x-ray diffraction pattern for one of the SL's, (GaAs)$_{17}$/(AlAs)$_{17}$, investigated in this work. This pattern was recorded in the vicinity of the (311) GaAs reflection using Cu$_{K_{\alpha 1}}$ radiation. The diffraction geometry is displayed in the inset of Fig. 6. The occurrence of sharp and distinct first-order satellite peaks $\pm$ 1 demonstrates the highly periodic structure of the SL. The parameters of the (GaAs)$_{n1}$/(AlAs)$_{n2}$ SL's determined from the spacing of these satellite peaks are (n1,n2)= (14,13), (17,17), (25,28), (27,25), (33,29), and (39,36) monolayers.

The Raman spectra were measured in backscattering geometry using a double grating spectrometer with Peltier-cooled photomultiplier and conventional photon counting. The lines between 4579 Å and 5145 Å of an Ar$^+$-ion laser were used as the incident radiation. During

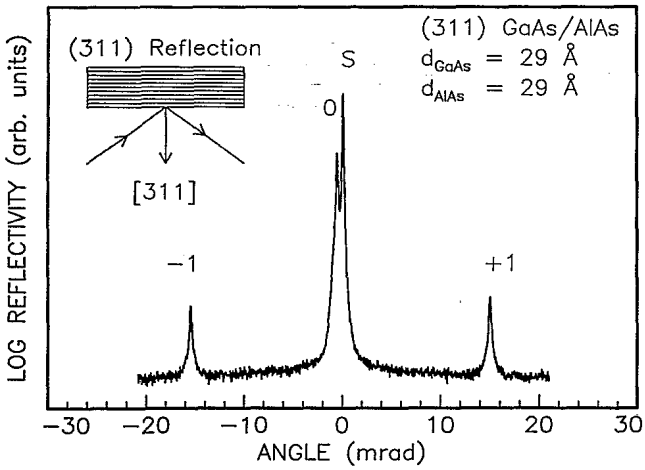

FIG. 6. X-ray diffraction pattern of the (311) $(GaAs)_{17}/(AlAs)_{17}$ SL measured with the $Cu_{K\alpha 1}$ line in the vicinity of the (311) reflection. S denotes the GaAs substrate peak and 0 and ± 1 the SL peaks.

the measurements the samples were maintained at liquid nitrogen temperature.

IV. RAMAN SPECTRA

A. Confined optical modes

Raman spectra of a (14,13) superlattice in the spectral region of GaAs (AlAs) optical phonons are given in Figs. 7 (and 8); Fig. 9 shows the GaAs frequency range of a (17,17) superlattice. From the symmetry properties of the eigenvectors it follows that the polarized spectra correspond to modes of A' symmetry, while the depolarized ones reflect modes of A'' symmetry. The corresponding Raman tensors and selection rules are given in Table I of Ref. 10. In the GaAs optical-phonon frequency region seven confined modes of A' symmetry are observed in the polarized spectra of the (14,13) SL in Fig. 7 and five A' modes in the case of the (17,17) SL in Fig. 9. The assignment of the observed modes, given in the upper part of Figs. 7 and 8, has been performed with the help of the calculated frequencies and eigenvectors described in Sec. III. The LO_m and $TO_{y',m}$ labeling implies the assigned dominant character of the eigenvectors. For the (17,17) SL the calculated eigenvector components of $LO_m (m=1-4)$ modes are given in Figs. 4(a)–4(d). The peak marked as $TO_{y',1}$ mode in Figs. 7 and 9 is the superposition of at least two modes whose eigenvector components are shown in Figs. 4(e) and 4(f).

The eigenvectors of the 267 cm^{-1} $TO_{y',m}$ mode for $m = 3$ are shown in Fig. 4(i). In the case of the AlAs optical-phonon region, Fig. 8 shows LO_m modes with indices up to $m = 5$. The mapping of these five frequencies onto the bulk dispersion indicates that there is much more dispersion in the AlAs bulk materials along [311] [Fig. 3(b)] than along the more commonly studied [001] direction. In the mass approximation the AlAs bulk

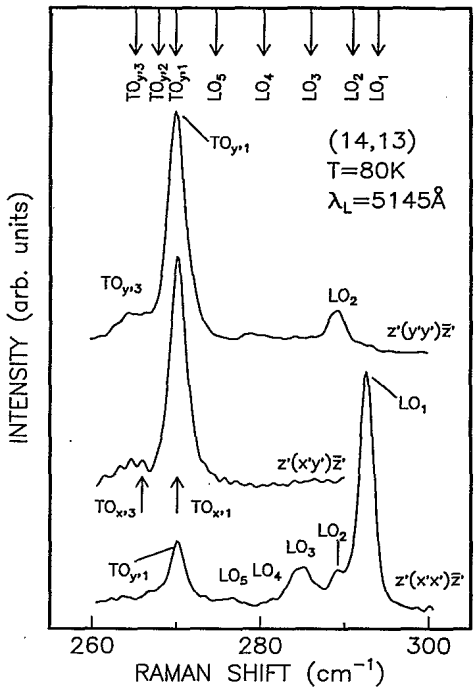

FIG. 7. Raman spectra of (311) $(GaAs)_{14}/(AlAs)_{13}$ SL at 80 K in backscattering configuration ($x' \parallel [01\bar{1}]$, $y' \parallel [\bar{2}33]$, $z' \parallel [311]$) measured with $\lambda_L = 5145$ Å . Calculated frequencies of the confined modes are indicated by arrows.

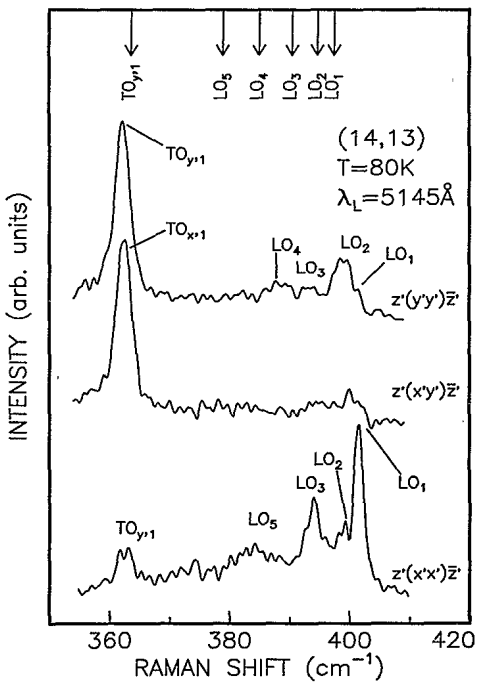

FIG. 8. Raman spectra of a (311) $(GaAs)_{14}/(AlAs)_{13}$ SL at 80 K in the optical-phonon region of AlAs measured with $\lambda_L = 5145$ Å. Calculated SL-mode frequencies are indicated by arrows.

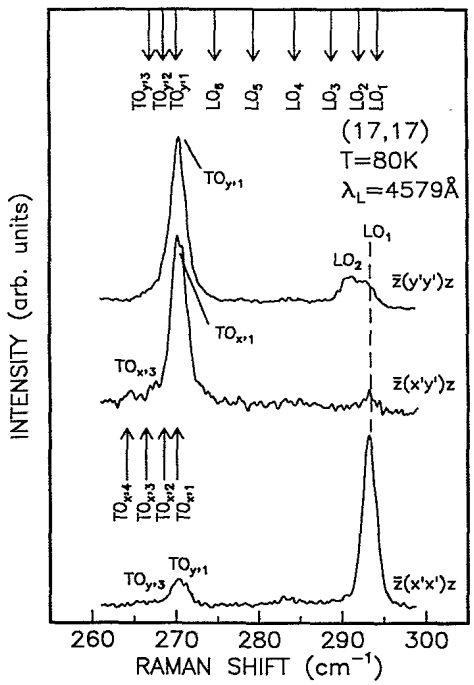

FIG. 9. Raman spectra of (311) $(GaAs)_{17}/(AlAs)_{17}$ superlattice at 80 K in backscattering configuration for $z'(y'y')\bar{z}'$, $z'(x'x')\bar{z}'$, and $z'(x'y')\bar{z}'$ polarizations with $\lambda_L = 4579$ Å. Calculated frequencies of the confined mode are indicated by arrows.

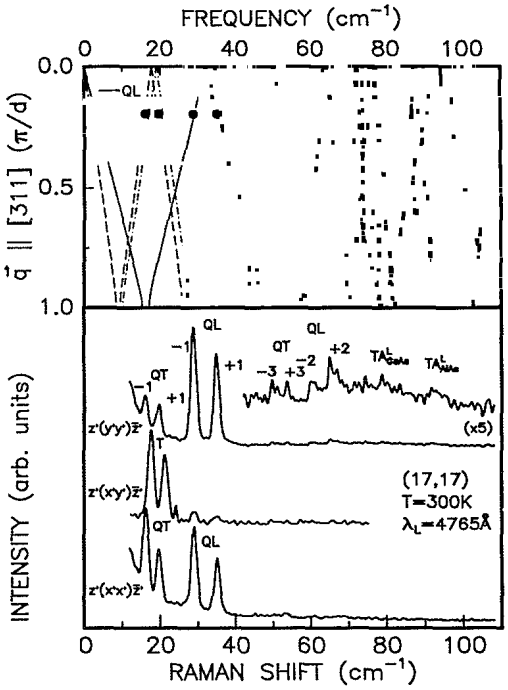

FIG. 10. Lower part: Raman spectra of a (311) $(GaAs)_{17}/(AlAs)_{17}$ SL in the spectral region from 10 to 110 cm^{-1} measured with 4765 Å at 300 K; upper part: shell model calculation for folded-phonon dispersion curves together with experimentally observed QL (•), QT (•), and T(○) folded phonons.

phonon frequencies are not exactly reproduced: along a cubic axis the whole LO branch is too low by about 6 cm^{-1} and the TO branches too high by about 4 cm^{-1} in comparison with a recent *ab initio* calculation of the AlAs dispersion.[18] If we shift our theoretical bulk dispersion curves along the [311] wave vector direction (and also the confined mode frequencies) to coincide with experimental data at the Γ point, the experimentally obtained frequencies of the AlAs-like confined modes map closely onto the optical bulk dispersion branches.

For the depolarized configuration we observe only $TO_{x',m}$ confined modes in agreement with the selection rules. In the AlAs optical phonon region (Fig. 8), however, only one such $TO_{x'}$ mode is resolved. In the GaAs optical phonon region (cf. Figs. 7 and 9) two such confined modes at about 270 cm^{-1} ($m = 1$) and 267 cm^{-1} ($m = 3$) are observed. The eigenvector component of the $TO_{x',1}$ mode at 270 cm^{-1} is shown in Fig. 3(g).

In the upper parts of Figs. 7–9 we compare the measured Raman spectra with the theoretical results. The calculated frequencies of the confined superlattice modes are represented by arrows. Good agreement between experimental and calculated frequencies of the confined optical modes is found for the (14,13) and (17,17) SL, especially in the GaAs region.

B. Folded acoustic phonons

In Fig. 10 we compare the frequencies of the measured folded-phonon modes of the (311) $(GaAs)_{17}/(AlAs)_{17}$ SL with calculations based on the shell model. It can be seen that folded phonons from all three acoustic branches are Raman active. In agreement with the polarization selection rules,[8] the quasitransverse (QT) and quasilongitudinal (QL) folded phonon doublets appear for parallel polarization configurations, while the purely transverse doublet is observed for crossed geometry. Besides the first-order doublets, two additional structures appear for parallel polarizations which we assign to the third QT and second QL doublets, since their positions agree with those predicted by the shell-model calculation. The broad features near 75 cm^{-1} and 90 cm^{-1} probably arise from SL and disorder-induced scattering by large wave vector TA phonons along $[01\bar{1}]$ and $[\bar{2}33]$ of GaAs and AlAs, respectively. We do not find any evidence of folded doublets resulting from the lateral periodicity, such as that recently reported by Belousov *et al.*[19] for SL's with similar parameters.

V. CONCLUSIONS

We have performed a shell-model calculation of the phonon frequencies and eigenvectors of (311) GaAs/AlAs SL's. The low crystal symmetry (C_s point group) of these SL's leads to vibrational properties. We find a strong mixing of the bulk $LO_{z'}$ and $TO_{y'}$ branches, which share A' symmetry with respect to the C_s point group. The confined optical modes of the SL are therefore superpositions of modes deriving from various bulk branches with

different effective wave vectors. However, we have shown that the dominant character of the SL modes can be determined by examining their calculated envelope function eigenvectors. The frequencies of both the confined optical and folded acoustic modes calculated for the SL's are in good agreement with those measured in the Raman spectra. We have also shown how the crystal symmetry effects the angular dispersion of the optic modes.

ACKNOWLEDGMENTS

We would like to thank H. Hirt, M. Siemers, and P. Wurster for expert technical help and M. Chamberlain for a careful reading of the manuscript. Z.V.P. and A.J.S. acknowledge financial support from the European Community and Royal Society (United Kingdom), respectively.

* Permanent address: Institut für Theoretische Physik, Universität Regensburg, D-93053 Regensburg, Germany. Present address: Department of Physics and Astronomy, Lexington, KY 40506-0055.

† Permanent address: Toshiba Cambridge Research Centre, Science Park, Milton Road, Cambridge CB4 4WE, United Kingdom.

‡ Permanent address: Paul-Drude-Institut für Festkörperelektronik, Hausvogteiplatz 5-7, 10117 Berlin, Germany.

[1] T. Fukunaga, T. Takamori, and H. Nakashima, J. Cryst. Growth **81**, 85 (1987).

[2] B. Gil, Y. El Khalifi, M. Mathieu, C. de Paris, J. Massies, G. Neu, T. Fukunaga, and H. Nakashima, Phys. Rev. B **41**, 2855 (1990).

[3] Y. El Khalifi, P. Lefebvre, J. Allegre, B. Gil, M. Mathieu, and T. Fukunaga, Solid State Commun. **75**, 677 (1990).

[4] R. Nötzel, N. N. Ledentsov, and K. Ploog, Phys. Rev. B **47**, 1299 (1993); R. Nötzel, N. N. Ledentsov, L. Däweritz, K. Ploog, and M. Hohenstein, *ibid.* **45**, 3507 (1992); R. Nötzel, L. Däweritz, and K. Ploog, *ibid.* **46**, 4736 (1992).

[5] E. C. Valadares, Phys. Rev. B **46**, 3995 (1992).

[6] A. T. Meney, Solid State Commun. **83**, 89 (1992).

[7] D. A. Contreras-Solorio, V. R. Velasco, and F. García-Moliner, Phys. Rev. B **47**, 4651 (1993).

[8] Z. V. Popović, J. Spitzer, T. Ruf, M. Cardona, R. Nötzel, and K. Ploog, Phys. Rev. B **48**, 1659 (1993).

[9] A. J. Shields, R. Nötzel, M. Cardona, L. Däweritz, and K. Ploog, Appl. Phys. Lett. **60**, 2537 (1992).

[10] A. J. Shields, Z. V. Popović, M. Cardona, J. Spitzer, R. Nötzel, and K. Ploog, following paper, Phys. Rev. B **49**, 7584 (1994).

[11] Z. V. Popović, M. Cardona, E. Richter, D. Strauch, L. Tapfer, and K. Ploog, Phys. Rev. B **40**, 1207 (1989).

[12] Z. V. Popović, M. Cardona, E. Richter, D. Strauch, L. Tapfer, and K. Ploog, Phys. Rev. B **43**, 4925 (1991).

[13] Z. V. Popović, M. Cardona, E. Richter, D. Strauch, L. Tapfer, and K. Ploog, Phys. Rev. B **40**, 3040 (1989).

[14] Z. V. Popović, M. Cardona, E. Richter, D. Strauch, L. Tapfer, and K. Ploog, Phys. Rev. B **41**, 5904 (1990).

[15] D. Strauch and B. Dorner, J. Phys. Condens. Matter **2**, 1457 (1990).

[16] G. Fasol, M. Tanaka, H. Sakaki, and Y. Horikashi, Phys. Rev. B **38**, 6056 (1988).

[17] C. Trallero-Giner, F. García-Moliner, V. R. Velasco, and M. Cardona, Phys. Rev. B **45**, 11 944 (1992); M. P. Chamberlain, M. Cardona, and B. K. Ridley, *ibid.* **48**, 14 356 (1993).

[18] S. Baroni, P. Giannozzi, and E. Molinari, Phys. Rev. B **41**, 3870 (1991).

[19] M. V. Belousov, V. Yu. Davydov, I. É. Kozin, P. S. Kop'ev, and N. N. Ledentsov, Pis'ma Zh. Eksp. Teor. Fiz. **57**, 112 (1993) [JETP Lett. **57**, 120 (1993)].